IEICE TRANS. COMMUN., VOL.E89–B, NO.11 NOVEMBER 2006

LETTER

A Novel Frequency Offset Estimation for OFDM Systems

Jong Yoon HWANG[†*], ***Student Member***, **Kwang Soon KIM**[†**a)], ***and*** **Keum-Chan WHANG**[†], ***Members***

SUMMARY In this letter, a blind frequency offset estimation algorithm is proposed for OFDM systems. The proposed method exploits the intrinsic phase shift between neighboring samples in a single OFDM symbol, incurred by a frequency offset. The proposed algorithm minimizes a novel cost function, which is the squared error of the candidate frequency offset compensated signals from two different observation windows. Also, the solution of the proposed algorithm is given by an explicit equation, which does not require any iterative calculation. It is shown that the performance of the proposed method is better than those of the conventional methods, especially in the presence of multipath channels. This is due to the fact that the proposed method is insensitive to inter-symbol interference (ISI).

key words: *blind synchronization, frequency offset estimation, orthogonal frequency division multiplexing (OFDM)*

1. Introduction

Orthogonal frequency division multiplexing (OFDM) is becoming more and more popular because it can support high data rate with high spectral efficiency. However, an OFDM system is very sensitive to the carrier frequency offset, which collapses the orthogonality between sub-carriers to degrade performance severely [1]. Among the many algorithms proposed for frequency offset estimation in OFDM systems [2]–[8], the most commonly used method is the cyclic prefix (CP)-based maximum likelihood estimation [2]. This CP-based ML algorithm exploits the redundant information in the CP and requires no training symbols. However, it suffers from the error floor since the CP may be severely corrupted in frequency selective fading channels. Schmidl and Cox proposed a training symbol based synchronization method [3] and Moose proposed an ML estimator using repeated data symbols [4]. These methods use the phase shifts between symbols, but need extra bandwidth. A blind method to find the frequency offset by using the intrinsic information in an OFDM symbol without any training sequence was proposed in [5]. However this method should be accompanied by oversampling. Other blind estimation methods such as in [6]–[8] need extra knowledge on the channel or suffer from high complexity. In this letter, we propose a novel blind estimation method for the frequency offset by exploiting the intrinsic phase shift incurred by the carrier frequency offset through time-shifted observation windows in an OFDM symbol. The key idea is that the phase difference between the signals of the two observation windows contains sufficient information for the frequency offset without any help of training sequence or oversampling mechanism.

Manuscript received October 26, 2005.

[†]The authors are with the Department of Electrical and Electronic Engineering, Yonsei University, 134 Shinchon-dong, Seodaemun-gu, Seoul, 120-749, Korea.

[*]The author is also with Telecommunication R&D Center, Samsung Electronics, Suwon-shi, Kyongki-do, Korea.

[**]Corresponding author.

a) E-mail: ks.kim@yonsei.ac.kr

DOI: 10.1093/ietcom/e89–b.11.3132

2. The Proposed Algorithm

For OFDM systems with N sub-carriers, an OFDM symbol is generated by using the inverse discrete-time Fourier transform (IDFT). In a time-dispersive channel with additive noise, the received continuous time baseband signal $y(t)$ is given by

$$y(t) = \frac{1}{\sqrt{N}} \sum_{k=0}^{N-1} x(k)H(k)e^{j2\pi(f_k+f_{off})t} + n(t), \tag{1}$$

where $x(k)$ and $H(k)$ are the information symbol and the channel response at the kth sub-carrier, respectively, f_k is the frequency of the kth sub-carrier, f_{off} is the frequency offset, and $n(t)$ is the complex Gaussian noise. By sampling with period of $T = T_s/N$, where T_s is the OFDM symbol interval without CP, we obtain two sets of discrete signals corresponding to the observation windows shown in Fig. 1 as

$$y_i(m) = \frac{1}{\sqrt{N}} \sum_{k=0}^{N-1} x(k)H(k)e^{j2\pi(k+\nu)\frac{1}{N}(m-\tau_i)} + n_i(m), \quad i = 1, 2, \tag{2}$$

where $\nu = f_{off}T_s$ is the normalized frequency offset. The above two sets of received time-domain signals can be written in more compact form by using matrix expression as

$$\mathbf{y}_i = e^{-j2\pi\nu\frac{\tau_i}{N}}\mathbf{\Gamma}(\nu)\mathbf{W}\mathbf{E}(\tau_i)\tilde{x} + \mathbf{n}_i, \quad i = 1, 2, \tag{3}$$

where $\Gamma(\nu) = \mathrm{diag}\left\{[\exp(j2\pi\nu m/N)]_{m=0}^{N-1}\right\}$, $\mathbf{E}(\tau) =$

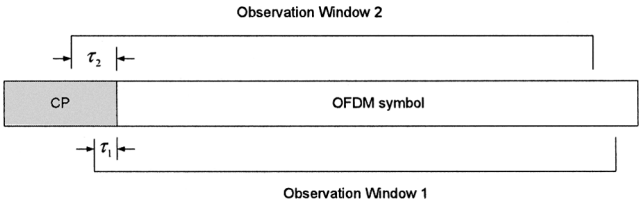

Fig. 1 Two observation windows with different delays.

$\mathrm{diag}\left\{\left[\exp(-j2\pi\tau k/N)\right]_{k=0}^{N-1}\right\}$, $\tilde{x} = \left([H(k)x(k)]_{k=0}^{N-1}\right)^T$, and $\mathbf{W}$ is the $N \times N$ IDFT matrix defined as

$$\mathbf{W} = \frac{1}{\sqrt{N}} \begin{bmatrix} 1 & 1 & \dots & 1 \\ 1 & e^{j2\pi\frac{1}{N}} & \dots & e^{j2\pi\frac{(N-1)}{N}} \\ \vdots & \vdots & \ddots & \vdots \\ 1 & e^{j2\pi\frac{(N-1)}{N}} & \dots & e^{j2\pi\frac{(N-1)(N-1)}{N}} \end{bmatrix}. \tag{4}$$

Here, $[a(m)]_{m=0}^{N-1}$ denotes a $1 \times N$ vector whose mth element is $a(m)$. Note that $\mathbf{\Gamma}(\nu)$ and $\mathbf{E}(\tau)$ represent intrinsic phase shifts caused by the carrier frequency offset and the timing offset, respectively. After compensating by a candidate frequency offset ν' in time-domain and performing DFT, we obtain the frequency-domain signal $\mathbf{Y}_1$ corresponding to the observation window 1 as

$$\mathbf{Y}_1 = \mathbf{W}^H \mathbf{\Gamma}^H(\nu')\mathbf{y}_1. \tag{5}$$

Similarly, we obtain the frequency-domain signal about the observation window 2 after the frequency offset compensation and DFT. There exists additional phase shift in $\mathbf{y}_2$ according to $\mathbf{E}(\tau_0)$ and $e^{-j2\pi\nu'\frac{\tau_0}{N}}$ compared to those in $\mathbf{y}_1$ due to the timing difference $\tau_0 = \tau_2 - \tau_1$ and the frequency offset ν. By compensating the above phase shift, we obtain another set of frequency-domain signal as

$$\mathbf{Y}_2^{(\tau_0)} = e^{j2\pi\nu'\frac{\tau_0}{N}} \mathbf{E}^H(\tau_0)\mathbf{W}^H\mathbf{\Gamma}^H(\nu')\mathbf{y}_2. \tag{6}$$

Note that $\mathbf{Y}_1 = \mathbf{Y}_2^{(\tau_0)}$, if there is no additive noise and $\nu = \nu'$. Then, the frequency offset is estimated by choosing ν' to minimize the difference between $\mathbf{Y}_1$ and $\mathbf{Y}_2^{(\tau_0)}$ as

$$\hat{\nu}(\tau_0) = \arg\min_{\nu'} \left\{\mathbf{Y}_1 - \mathbf{Y}_2^{(\tau_0)}\right\}^H \left\{\mathbf{Y}_1 - \mathbf{Y}_2^{(\tau_0)}\right\}. \tag{7}$$

We developed this algorithm from the intuition that only the difference between signals from windows 1 and 2 after DFT is phase shift due to the frequency offset and timing shift. So, we can find the frequency offset by compensating the phase shift corresponding timing shift. One thing we should note is that the candidate frequency offset compensation should be done before DFT to avoid inter-carrier interference.

Now we think of the cost function in (7) to reduce the searching complexity. After some mathematical calculation shown in Appendix, the cost function can be expressed as a function of candidate frequency offset ν' as

$$\begin{aligned} S^{(\tau_0)}(\nu') &= \left\{\mathbf{Y}_1 - \mathbf{Y}_2^{(\tau_0)}\right\}^H \left\{\mathbf{Y}_1 - \mathbf{Y}_2^{(\tau_0)}\right\} \\ &= A - B\cos\{2\pi(\nu - \nu' - q)\}, \end{aligned} \tag{8}$$

where A, B and q depend on data and noise, but are independent to the candidate frequency offset. The frequency offset estimate $\hat{\nu}$, which makes the cost function minimum, is apparently $\nu - q$. Here, q is dependent on noise and deteriorates the performance of the estimator. From (8), we can obtain an explicit expression for the frequency offset estimator as follows. Since we have three unknown variables in (8), for any given three values, ν'_1, ν'_2, and ν'_3, the ratio of the difference of the cost function is given as

$$\begin{aligned} &\frac{S^{(\tau_0)}\left(\nu'_3\right) - S^{(\tau_0)}\left(\nu'_1\right)}{S^{(\tau_0)}\left(\nu'_3\right) - S^{(\tau_0)}\left(\nu'_2\right)} \\ &\quad = \frac{\sin\left\{2\pi\hat{\nu}(\tau_0) - \pi\left(\nu'_3 + \nu'_1\right)\right\}\sin\left\{\pi\left(\nu'_1 - \nu'_3\right)\right\}}{\sin\left\{2\pi\hat{\nu}(\tau_0) - \pi\left(\nu'_3 + \nu'_2\right)\right\}\sin\left\{\pi\left(\nu'_2 - \nu'_3\right)\right\}}, \end{aligned} \tag{9}$$

where $\hat{\nu}(\tau_0) = \nu - q$. Let's define $\rho^{(\tau_0)}$ as

$$\rho^{(\tau_0)} \triangleq \frac{S^{(\tau_0)}\left(\nu'_3\right) - S^{(\tau_0)}\left(\nu'_1\right)}{S^{(\tau_0)}\left(\nu'_3\right) - S^{(\tau_0)}\left(\nu'_2\right)} \cdot \frac{\sin\left\{\pi\left(\nu'_2 - \nu'_3\right)\right\}}{\sin\left\{\pi\left(\nu'_1 - \nu'_3\right)\right\}}. \tag{10}$$

Substituting (10) into (9) and using trigonometric manipulation, the frequency offset estimator is given by

$$\hat{\nu}(\tau_0) = \frac{1}{2\pi}\tan^{-1}\frac{\sin\left\{\pi\left(\nu'_3 + \nu'_1\right)\right\} - \rho^{(\tau_0)}\sin\left\{\pi\left(\nu'_3 + \nu'_2\right)\right\}}{\cos\left\{\pi\left(\nu'_3 + \nu'_1\right)\right\} - \rho^{(\tau_0)}\cos\left\{\pi\left(\nu'_3 + \nu'_2\right)\right\}}. \tag{11}$$

As will be seen in the simulation results, the performance of the proposed frequency offset estimator in (11) gets better as τ_0 increases as long as the observation window 2 is not corrupted by the previous symbol in a frequency selective fading channel. This comes from the fact that the phase rotation caused by a given frequency offset ν becomes larger as τ_0 increases, which increases the difference between $\mathbf{Y}_1$ and $\mathbf{Y}_2^{(\tau_0)}$, and improves the performance of the proposed estimator. However, if τ_0 is set too large, the performance of the proposed frequency offset estimator suffers from error floor due to ISI. Thus, it is desirable to increase τ_0 until $T_{cp} - \tau_2$ remains greater than the largest delay of the multipath channel, where T_{cp} is the length of the cyclic prefix. Since the optimal value of τ_0 depends on channel environment and even varies with time, we propose another blind frequency offset estimator as

$$\begin{aligned} \hat{\nu} &= \frac{1}{K}\sum_{k=1}^{K}\hat{\nu}(k) = \frac{1}{2\pi K}\sum_{k=1}^{K}\tan^{-1} \\ &\quad \cdot \frac{\sin\left\{\pi\left(\nu'_3 + \nu'_1\right)\right\} - \rho^{(k)}\sin\left\{\pi\left(\nu'_3 + \nu'_2\right)\right\}}{\cos\left\{\pi\left(\nu'_3 + \nu'_1\right)\right\} - \rho^{(k)}\cos\left\{\pi\left(\nu'_3 + \nu'_2\right)\right\}}, \end{aligned} \tag{12}$$

where K is a design parameter not greater than the system's guard interval. In the next section, we will show that the estimator proposed at (12) is robust to ISI and relieves the difficulty to find proper value of τ_0.

3. Simulation Results

The performance of the proposed estimator is compared with the CP-based ML estimator [2] with perfect timing synchronization and the oversampling algorithm [5] at various frequency selective fading channels. We use the normalized mean square error (MSE) of the estimator as a performance measure, which is the variance of the estimated normalized

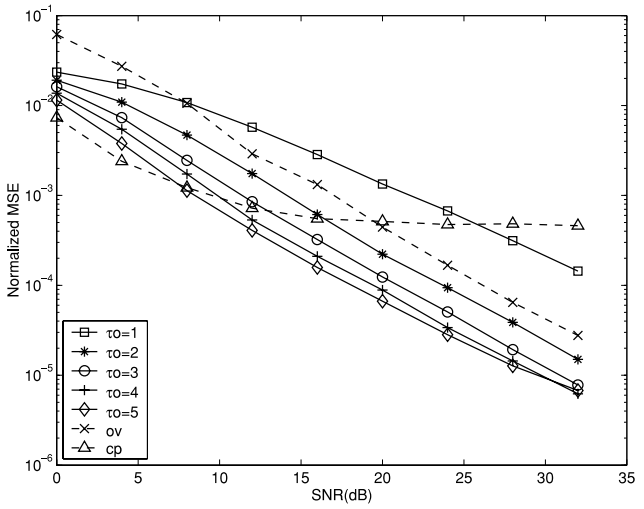

Fig. 2 Normalized MSE of frequency offset estimation of various blind algorithms in a dispersive channel.

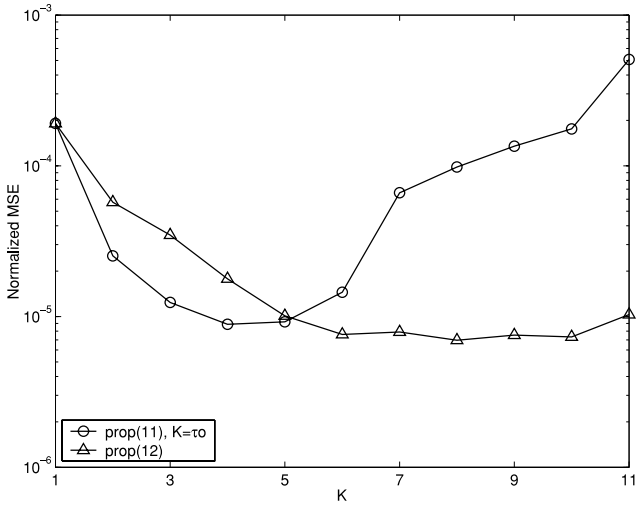

Fig. 3 Performance variations of the estimators as a function of difference between observation windows and averaging interval at 30 dB SNR of a dispersive channel.

carrier frequency offset ($\hat{\nu}$). For simulation parameters, the number of sub-carriers, N, is 64, the length of the CP is 11 samples, and the maximum delay of the frequency selective fading channel is set to 9 samples, respectively. A nine-tap multipath channel is generated with exponentially decaying power delay profile. As we can see in Fig. 2, the proposed method in (11) with appropriate selection of parameters shows better performance than the conventional methods. The CP-based method (cp) suffers from an error floor due to the corrupted CP in a multipath fading channel. Mostly the proposed method shows better performance than the oversampling method (ov) due to the larger phase rotations between the signals from the two observation windows, and gets better as τ_0 increases. As mentioned before, too large value of τ_0 may degrade the performance of the estimator due to ISI. Figure 3 depicts the performance variation of the proposed estimator at 30 dB of SNR as a function of K to show the ISI effect, where K is the difference between the observation windows for the estimator in (11), namely τ_0, and the averaging interval in (12). As shown in the figure, the method in (12) is nearly insensitive to the ISI and shows pretty good performance over entire range of K. Figure 4 shows the performances of the proposed method (prop) in (12) with $K = 9$, the oversampling method and the CP-based method with perfect timing in three different dispersive channels: i) a nine-path channel with exponentially decaying power profile (solid lines), ii) a nine-path channel with uniform power profile (dash-doted lines), and iii) a fourteen path channel with exponentially decaying power profile (dotted lines). Note that the maximum delay of the third channel is greater than the CP length. As can be seen from the figure, the proposed estimator outperforms the other algorithms in various multipath fading channels. All three algorithms show error floors at high SNR caused by ISI in the channel (iii). However, even in that case, the proposed algorithm is less influenced by ISI and results in superior performance than the other two methods.

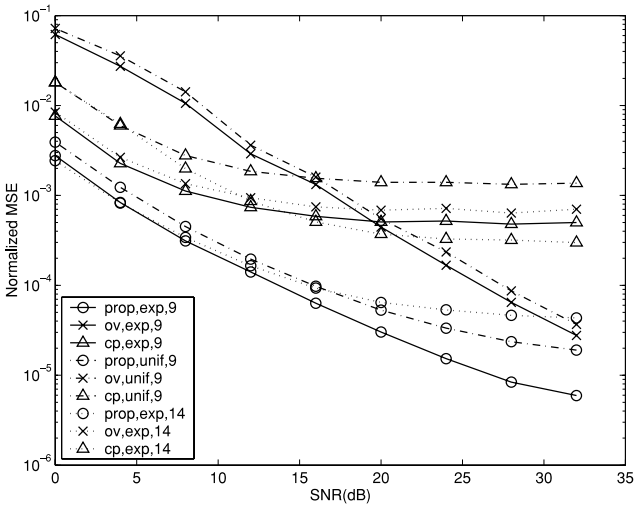

Fig. 4 Normalized MSE of frequency offset estimation of various blind algorithms in three different dispersive channels.

4. Conclusion

In this letter, we proposed a novel carrier frequency offset estimation algorithm for OFDM systems by using the intrinsic phase shift between the samples at one OFDM symbol. The phase shift induced by carrier frequency offset is easily measured by comparing the phase shift between the two sets of samples from different observation windows without any kind of oversampling mechanism. An efficient method to find the minimum of the cost function is derived and eliminates the searching complexity. The proposed algorithm shows robustness to ISI and provide much better estimation performance than the CP-based method and the oversampling method in multipath fading channels using just one OFDM symbol.

References

[1] T. Pollet, M. Van Bladel, and M. Moeneclaey, "BER sensitivity of OFDM systems to carrier frequency offset and Wiener phase noise," IEEE Trans. Commun., vol.43, no.2/3/4, pp.191–193, Feb./March/April 1993.
[2] J. van de Beek, M. Sandell, and P.O. Börjesson, "ML estimation of time and frequency offset in OFDM systems," IEEE Trans. Signal Process., vol.45, no.7, pp.1800–1805, July 1997.
[3] T.M. Schmidl and D.C. Cox, "Robust frequency and timing synchronization for OFDM," IEEE Trans. Commun., vol.45, no.12, pp.1613–1621, Feb. 1997.
[4] P. Moose, "A technique for orthogonal frequency division multiplexing frequency offset correction," IEEE Trans. Commun., vol.42, no.10, pp.2908–2914, Oct. 1994.
[5] B. Chen and H. Wang, "Blind estimation of OFDM carrier frequency offset via oversampling," IEEE Trans. Signal Process., vol.52, no.7, pp.2047–2057, July 2004.
[6] H. Bölcskei, "Blind estimation of symbol timing and carrier frequency offset in wireless OFDM systems," IEEE Trans. Commun., vol.49, no.6, pp.988–998, June 2001.
[7] H. Liu and U. Tureli, "A high-efficiency carrier estimator for OFDM communications," IEEE Commun. Lett., vol.2, no.4, pp.104–106, April 1998.
[8] U. Tureli, H. Liu, and M. Zoltowski, "OFDM blind carrier offset estimation: ESPRIT," IEEE Trans. Commun., vol.48, no.9, pp.1459–1461, Sept. 2000.

Appendix: Derivation of Eq. (8)

We rewrite the received discrete time baseband signal from each observation windows as

$$y_i(m) = d_i(m) + n_i(m), \tag{A·1}$$

where $d_i(m)$ is data dependent part of $y_i(m)$ in (2). Let's denote the pth element of $N \times 1$ vector $\mathbf{Y}_i$ as Y_{ip}, and

$$Y_{1p} = \frac{1}{\sqrt{N}} \sum_{m=0}^{N-1} \{d_1(m) + n_1(m)\} e^{-j2\pi(\nu'+p)\frac{m}{N}} \tag{A·2}$$

and

$$Y_{2p} = \frac{1}{\sqrt{N}} \sum_{m=0}^{N-1} \{d_2(m) + n_2(m)\} e^{-j2\pi(\nu'+p)\frac{(m-\tau_0)}{N}}. \tag{A·3}$$

Using cyclic property of the signals, Y_{2p} can be rewritten as

$$\begin{aligned} Y_{2p} &= \frac{1}{\sqrt{N}} \sum_{m=0}^{\tau_0-1} \{d_2(m) + n_2(m)\} e^{-j2\pi(\nu'+p)\frac{(m-\tau_0)}{N}} \\ &\quad + \frac{1}{\sqrt{N}} \sum_{m=\tau_0}^{N-1} \{d_2(m) + n_2(m)\} e^{-j2\pi(\nu'+p)\frac{(m-\tau_0)}{N}} \\ &= \frac{1}{\sqrt{N}} \sum_{m=N-\tau_0}^{N-1} \left\{ d_1(m) e^{-j2\pi\nu} + n_2(m-N+\tau_0) \right\} \\ &\quad \cdot e^{-j2\pi(\nu'+p)\frac{(m-N)}{N}} \\ &\quad + \frac{1}{\sqrt{N}} \sum_{m=0}^{N-1-\tau_0} \{d_1(m) + n_1(m)\} e^{-j2\pi(\nu'+p)\frac{m}{N}}. \end{aligned} \tag{A·4}$$

The difference between Y_{1p} and Y_{2p} is given by

$$\begin{aligned} Y_{1p} - Y_{2p} &= \frac{1}{\sqrt{N}} \sum_{m=N-\tau_0}^{N-1} \left\{ d_1(m) \left(1 - e^{-j2\pi(\nu-\nu')}\right) \right. \\ &\quad \left. + \alpha(m) \right\} e^{-j2\pi(\nu'+p)\frac{m}{N}}, \end{aligned} \tag{A·5}$$

where $\alpha(m) \triangleq n_1(m) - n_2(m - N + \tau_0) e^{j2\pi\nu'}$. Thus, the cost function of the estimator is given by

$$\begin{aligned} S(\nu') &= \{\mathbf{Y}_1 - \mathbf{Y}_2\}^H \{\mathbf{Y}_1 - \mathbf{Y}_2\} \\ &= \sum_{m=N-\tau_0}^{N-1} \left\{ |d_1(m)|^2 \cdot \left|1 - e^{-j2\pi(\nu-\nu')}\right|^2 \right. \\ &\quad + 2Re\left\{ d_1(m)\alpha^*(m) \left(1 - e^{-j2\pi(\nu-\nu')}\right) \right\} \\ &\quad \left. + |\alpha(m)|^2 \right\}. \end{aligned} \tag{A·6}$$

Here, we omit the superscript (τ_0) in $\mathbf{Y}_2$ and $S(\nu')$ for simplicity. Let's define $\tilde{d}_1^T = [d_1(m)]_{m=N-\tau_0}^{N-1}$, $\tilde{n}_1^T = [n_1(m)]_{m=N-\tau_0}^{N-1}$, $\tilde{n}_2^T = [n_2(m)e^{j2\pi\nu}]_{m=0}^{\tau_0-1}$, $\tilde{\alpha}^T = [\alpha(m)]_{m=N-\tau_0}^{N-1}$, and $\theta = 2\pi(\nu-\nu')$. After some mathematical manipulation, the terms in (A·6) can be represented as $\sum_{m=N-\tau_0}^{N-1} |\alpha(m)|^2 = \|\tilde{\alpha}\|^2 = C_1 - C_2\cos(\theta - \psi_1)$ and $\sum_{m=N-\tau_0}^{N-1} Re\left\{d_1(m)\alpha^*(m)(1 - e^{-j\theta})\right\} = C_3 - C_4\cos(\theta - \psi_2)$, where $C_1 = \|\tilde{n}_1\|^2 + \|\tilde{n}_2\|^2$, $C_2 = 2|\tilde{n}_1^H \tilde{n}_2|$, $\psi_1 = \angle(\tilde{n}_1^H \tilde{n}_2)$, $C_3 = Re\{(\tilde{n}_1 + \tilde{n}_2)^H \tilde{d}_1\}$, $C_4 = |\tilde{d}_1^H \tilde{n}_1 + \tilde{n}_2^H \tilde{d}_1|$, and $\psi_2 = \angle(\tilde{d}_1^H \tilde{n}_1 + \tilde{n}_2^H \tilde{d}_1)$. Note that $C_1, C_2, C_3, C_4, \psi_1$ and ψ_2 are real-valued and independent to the candidate frequency offset ν'. Then the cost function can be expressed as

$$\begin{aligned} S(\nu') &= \|\tilde{d}_1\|^2(2 - 2\cos\theta) + C_1 - C_2\cos(\theta - \psi_1) \\ &\quad + 2C_3 - 2C_4\cos(\theta - \psi_2) \\ &= A - B\cos\{2\pi(\nu - \nu' - q)\}, \end{aligned} \tag{A·7}$$

where $A = 2\|\tilde{d}_1\|^2 + \|\tilde{n}_1\|^2 + \|\tilde{n}_2\|^2 + 2Re\{(\tilde{n}_1 + \tilde{n}_2)^H \tilde{d}_1\}$, $B = 2\left|\|\tilde{d}_1\|^2 + \tilde{n}_1^H \tilde{n}_2 + \tilde{d}_1^H \tilde{n}_1 + \tilde{n}_2^H \tilde{d}_1\right| > 0$, and $q = 1/2\pi\angle\{\|\tilde{d}_1\|^2 + \tilde{n}_1^H \tilde{n}_2 + \tilde{d}_1^H \tilde{n}_1 + \tilde{n}_2^H \tilde{d}_1\}$. Thus, the cost function is minimized at $\nu' = \hat{\nu} = \nu - q$.